Magnetic properties of the helimagnet $Cr_{1/3}NbS_2$ observed by μSR

D. Braam,[1] C. Gomez,[1] S. Tezok,[1] E. V. L. de Mello,[2] L. Li,[3] D. Mandrus,[3,4] Hae-Young Kee,[5,6] and J. E. Sonier[1,6]

[1]*Department of Physics, Simon Fraser University, Burnaby, British Columbia V5A 1S6, Canada*

[2]*Instituto de Física, Universidade Federal Fluminense, Niterói RJ 24210-340, Brazil*

[3]*Department of Materials Science and Engineering, University of Tennessee, Knoxville, Tennessee 37996, USA*

[4]*Oak Ridge National Laboratory, Oak Ridge, Tennessee 37831, USA*

[5]*Department of Physics, University of Toronto, Ontario M5S 1A7, Canada*

[6]*Canadian Institute for Advanced Research, Toronto, Ontario M5G 1Z8, Canada*

We have performed muon spin rotation and relaxation (μSR) measurements on single crystals of the chiral helimagnet $Cr_{1/3}NbS_2$ at zero to low magnetic field. The transition from the paramagnetic to helical magnetically ordered phase at zero field is marked by the onset of a coherent oscillation of the zero-field muon spin polarization below a critical temperature T_c. An enhancement of the muon spin precession frequency is observed below $T \sim$ 50 K, where anomalous behavior has been observed in bulk transport measurements. The enhanced precession frequency indicates a low-temperature modification of the helical magnetic structure. A Landau free-energy analysis suggests that the low-temperature change in the magnetic structure is caused by a structural change. We also suggest a longer periodicity of helicity below $T \sim$ 50 K, which can be verified by neutron-scattering experiments.

$Cr_{1/3}NbS_2$ is an itinerant chiral helimagnet (CHM) with a hexagonal noncentrosymmetric crystal structure [1]. In crystals belonging to a noncentrosymmetric space group, CHM order is generally understood to be a consequence of competing symmetric Heisenberg exchange and Dzyaloshinsky-Moriya (DM) interactions. The CHM order in $Cr_{1/3}NbS_2$ continuously evolves into an incommensurate chiral magnetic soliton lattice (CSL) upon application of a magnetic field perpendicular to the helical c axis ($\mathbf{H} \perp \hat{c}$) [2,3]. The CSL consists of periodic domains of ferromagnetically ordered spins in the ab plane separated by 360° spin domain walls. The period of the CSL increases monotonically with the magnitude of the applied field, resulting in a continuous phase transition to a commensurate ferromagnetic (FM) state. The ability to easily tune the size of the magnetic domains of the CSL, and hence the magnetic potential experienced by the spins of the itinerant electrons, makes $Cr_{1/3}NbS_2$ an appealing candidate for spintronics applications.

At elevated temperatures there is a transition to a paramagnetic (PM) state. Reported values of the PM-to-CHM phase transition temperature T_c vary between 118 K [4] and 133.5 K [5]. While the long-range magnetically ordered phases of $Cr_{1/3}NbS_2$ have been established, the details of the transition from the PM phase to the CHM or CSL phases are unresolved. Anomalies in the magnetic field dependence of the resistivity and the temperature dependences of the Seebeck and Hall coefficients near T_c have been reported [6,7]. In particular, at T_c a significant negative magnetoresistance (with $\mathbf{H} \perp \hat{c}$) has been observed, with no saturation of the resistivity at fields where both the resistivity and magnetization saturate at lower temperatures [6]. The Seebeck and Hall coefficients also show a pronounced minimum near T_c, indicative of changes to the electronic structure and/or the effects of the magnetism on the mobility of the charge carriers. Likewise, anomalous behavior has been observed in magnetoresistance, thermopower, and Hall resistivity data below $T \sim$ 50 K [5]. At these low

temperatures the magnetoresistance at high fields becomes anisotropic, there is a rapid decrease of the Seebeck coefficient with decreasing temperature, and the field dependence of the Hall resistivity drastically changes. To gain further insight into the sources of the transport anomalies, we have used the μSR technique to investigate the nature of the accompanying magnetism.

Our μSR measurements were performed at TRIUMF on a $\sim$50-mm² mosaic consisting of seven $\sim$0.25-mm-thick platelike $Cr_{1/3}NbS_2$ single crystals, which were grown as described in Ref. [6]. The positive muon (μ^+) beam was directed at the large face of the mosaic, with the linear momentum of the beam parallel to the c axis of the crystals (z direction). The initial muon spin polarization $\mathbf{P}(t=0)$ for all measurements was rotated to be perpendicular to the c axis (x direction). Data were collected with zero applied magnetic field (ZF) and for a transverse field (TF) [i.e., perpendicular to $\mathbf{P}(t=0)$] applied perpendicular to the c axis (y direction). Note that for the desired $\mathbf{H} \perp \hat{c}$ orientation the field must be applied perpendicular to the beam, since the crystals are too thin to orient with the beam shining on the a-c or b-c plane faces. The ensuing beam deflection by the magnetic force exerted on the incoming μ^+ limited the applied field strength to $H \leqslant$ 600 Oe.

Figure 1(a) shows representative ZF-μSR asymmetry spectra. The data for $135 \leqslant T \leqslant 170$ K were best fit to

$$A(t) = \sum_{i=1}^{2} A_i G_{KT}(\Delta_i, t)e^{-\lambda t} + A_b, \quad (1)$$

where $G_{KT}(\Delta_i, t)$ is a static Gaussian Kubo-Toyabe relaxation function and A_b is a small time-independent background signal. The fits yield $A_1/A_2 \approx 2$, $\Delta_1 = 0.091(4)$ μs⁻¹, $\Delta_2 = 0.414(5)$ μs⁻¹, and a relaxation rate λ that exhibits a divergent increase as the temperature is lowered. Based on these results and nuclear dipole field calculations, we attribute the two sample components to a muon stopping site near a S atom
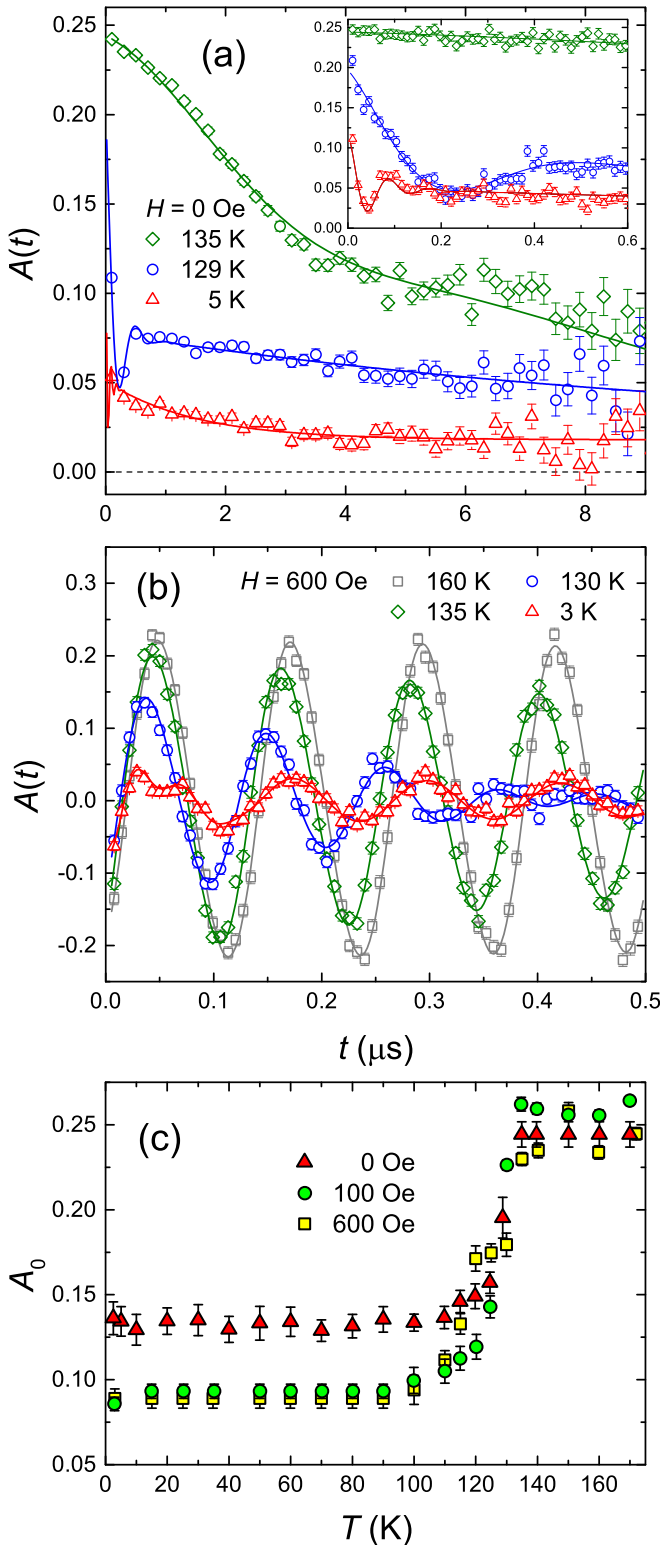
FIG. 2. (Color online) Simulations of the sample(s) contribution to the ZF-μSR signal for $Cr_{1/3}NbS_2$ in the CHM ground state. The dashed curves show the contribution from muons stopping near Nb at $(0.77, 0.32, 0.96)$ and near S at $(0.37, 0.78, 0.6)$, where the coordinate values are multiples of the respective lattice constants $a = b = 5.7$ Å and $c = 12.1$ Å. The Cr magnetic moment is assumed to be 4.4 μ_B. The occupation probability of the muon site near S is taken to be twice that of the site near Nb.

and a site near Nb. The amplitude ratio A_1/A_2 implies that the probability of the muon stopping at the S site is approximately twice that of the Nb site.

For $T \leqslant 130$ K the relaxation rate is sufficiently fast that some of the measured ZF-μSR signal is damped out in the initial dead time of the μSR spectrometer, resulting in a reduction of the initial amplitude $A_0 = A_1 + A_2 + A_b$ [see Fig. 1(c)]. The asymmetry spectra at these temperatures were fit to

$$A(t) = A_1 e^{-\Lambda_1 t} \cos(2\pi f t) + A_2 e^{-\Lambda_2 t} + A_b. \quad (2)$$

The oscillating term is indicative of magnetic order, and the spin precession frequency f is related to the magnitude of the mean field B_μ sensed by the muon ensemble, where $f = (\gamma_\mu/2\pi) B_\mu$ and $\gamma_\mu/2\pi = 135.54$ MHz/T is the muon gyromagnetic ratio. Despite there being two muon stopping sites, we could not resolve two distinct frequencies. This is understandable from simulations of the contribution of each of these sites to the ZF-μSR signal (see Fig. 2), where the signal from muons stopping near Nb is smaller and rapidly damped. The temperature dependence of f indicates a magnetic transition at $T_c = 129.6$ K (see Fig. 3), which is close to previous estimates of the Curie temperature of $Cr_{1/3}NbS_2$ [1].

Figure 1(b) shows representative TF-μSR spectra for $\mathbf{H} \perp \hat{c}$ and $H = 600$ Oe. The external field adds vectorially to the local field generated by the spin structure. At all temperatures the TF-μSR spectrum is well described by the sum of the sample and background contribution of the following form:

$$A(t) = A_s e^{-\Lambda t} \cos(2\pi f t) + A_b e^{-\sigma^2 t^2} \cos(2\pi f_b t), \quad (3)$$

where $A_0 = A_s + A_b$ is the total signal amplitude. There is a rapid signal depolarization below T_c, which manifests itself in a reduction of A_0 that is more severe than with $H = 0$ [see

FIG. 1. (Color online) (a) Representative ZF-μSR asymmetry spectra of $Cr_{1/3}NbS_2$ recorded at different temperatures. The inset shows the asymmetry spectra at early times, with the data packed into smaller time bins. The solid curves through the data points are fits to Eqs. (1) and (2). (b) Representative TF-μSR asymmetry spectra of $Cr_{1/3}NbS_2$ recorded at different temperatures with $H = 600$ Oe. The solid curves through the data points are fits to Eq. (3). (c) Temperature dependence of the total initial asymmetry A_0.
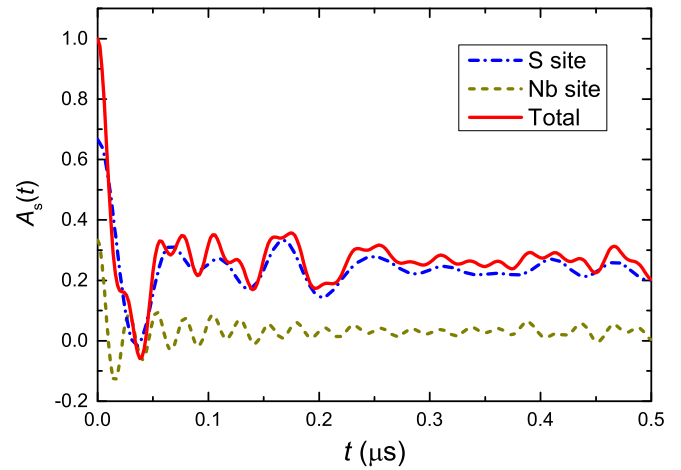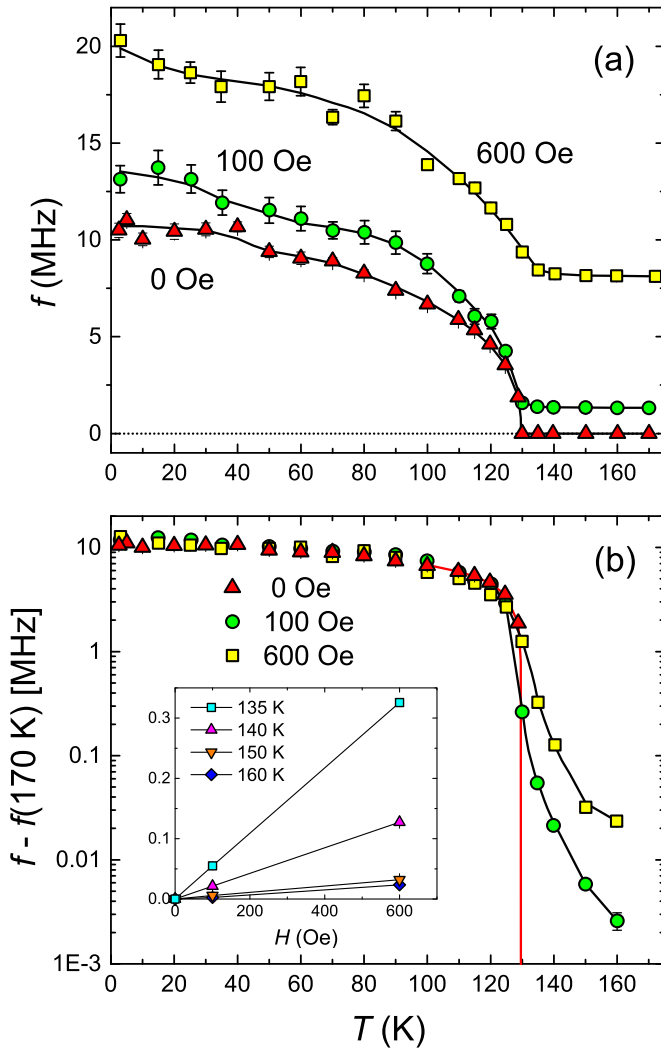
FIG. 3. (Color online) Temperature dependence of (a) the muon spin precession frequency f observed for different applied magnetic field strengths and of (b) the frequency shift $f(T) - f(T = 170\ K)$ plotted with a logarithmic vertical scale. The black solid curves through the data points in both panels are guides to the eye. The red curve in (b), which extends off the logarithmic scale, comes from a fit of the high-temperature data for $H = 0$ Oe to $f(T) = f(0)(1 - T/T_c)^n$, yielding $T_c = 129.58(4)$ K and $n = 0.366(6)$. The inset shows the magnetic field dependence of $f(T) - f(T = 170\ K)$ at temperatures above T_c.

Fig. 1(c)]. Bulk magnetization measurements suggest that the CSL state is not fully formed until $H \approx 850$ Oe [6]. A distortion of the CHM order into an inhomogeneous helicoid is consistent with the enhanced depolarization observed here at weaker fields. As shown in Fig. 3(a), the temperature dependence of the spin precession frequency f is similar to that observed with $H = 0$, but shifted in value by the applied field. There is some enhancement of f at low temperatures, which is indicative of a structural change and/or modification of the spin structure. At $H = 0$ Oe and $H = 100$ Oe this occurs below $T \approx 50$ K, where as mentioned earlier, anomalous behavior has been observed in transport measurements.

Figure 3(b) shows the temperature dependence of the frequency difference $f(T) - f(T = 170\ K)$. With $H > 0$, the

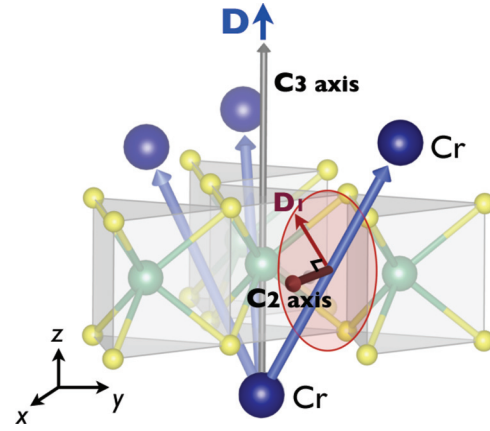FIG. 4. (Color online) Illustration of the DM interaction in $Cr_{1/3}NbS_2$. Each Cr atom (blue spheres) is linked to three Cr atoms in one of the adjacent planes (indicated by the blue arrows). The S and Nb atoms are the yellow and green spheres, respectively. The cylindrical red arrow represents a C_2 rotational symmetry axis located halfway between the two Cr atoms. The DM vector $\mathbf{D}_1$ linking these two Cr atoms (flat red arrow) lies in the red-shaded plane perpendicular to the C_2 axis. Note that the precise orientation of $\mathbf{D}_1$ in the red-shaded plane is unknown. The related DM vectors $\mathbf{D}_2$ and $\mathbf{D}_3$ linking the lower Cr atom with the other two Cr atoms in the upper layer are not shown. The gray arrow represents a C_3 rotational symmetry axis relating the three Cr atoms in the upper layer. The short blue arrow above this is the resultant DM vector $\mathbf{D} = \mathbf{D}_1 + \mathbf{D}_2 + \mathbf{D}_3$.

spin precession frequency increases as the zero-field magnetic transition temperature T_c is approached from above. As shown in the inset of Fig. 3(b), $f(T) - f(T = 170\ K) \propto H$ at temperatures $T_c < T < 170$ K, where the proportionality constant is roughly proportional to $1/(T - T_c)$. Hence the observed frequency shift above T_c is consistent with the low-field response of a paramagnet, whereby the induced magnetization is linearly dependent on H. A full and temperature-independent amplitude A_0 is observed above T_c [see Fig. 1(b)], indicating that the paramagnetism occurs throughout the sample volume.

To provide a possible explanation for the enhanced mean magnetic field sensed by the muon ensemble ($\sim f$) at low temperatures, we adopt a Landau free-energy analysis. In the absence of the $\mathbf{H} \perp \hat{c}$ magnetic field, the helimagnetic phase occurs via FM and DM interactions due to a lack of inversion symmetry. As shown in Fig. 4, the Cr atoms form layered triangular lattices in $Cr_{1/3}NbS_2$, with a hexagonal space group of $P6_322$. For each Cr atom in a layer, there are three nearest-neighbor Cr atoms in an adjacent layer. C_2 rotational symmetry exists about an axis located halfway between two Cr atoms in the different layers, with inversion symmetry about this point broken by the S atoms. The DM vector linking the two Cr atoms ($\mathbf{D}_1$) then lies in a plane perpendicular to the C_2 axis, as shown in Fig. 4. Since the three Cr atoms within a layer are related by C_3 rotational symmetry (about an axis parallel to the z axis), there are three DM vectors related by symmetry ($\mathbf{D}_1$, $\mathbf{D}_2$, and $\mathbf{D}_3$), which when summed together give a resultant DM vector $\mathbf{D}$ pointing along the z axis. Consequently, the spin density of the helical order can be described by [8,9]

$$\mathbf{S}(\mathbf{r}) = \mathbf{S} \exp(i\mathbf{Q} \cdot \mathbf{r}) + \mathbf{S}^* \exp(-i\mathbf{Q} \cdot \mathbf{r}), \quad (4)$$

where $\mathbf{Q} = Q_0\hat{z}$, $\mathbf{S} = S_x\hat{x} + iS_y\hat{y}$, and by symmetry $|S_x| = |S_y| \equiv S$. Since the free energy should be invariant under the exchange of $\mathbf{Q} \to -\mathbf{Q}$ and $\mathbf{S} \to -\mathbf{S}^*$, it is given to fourth order by [8,9]

$$F = \alpha_0 \mathbf{S} \cdot \mathbf{S}^* + DQ_0 S^2 + \alpha_1 Q_0^2 S^2 + \beta S^4, \qquad (5)$$

where D represents the strength of the DM interaction [10], and the parameter β is assumed to be positive, such that the free energy is bound. Minimizing F with respect to Q_0, we find $Q_0 = -D/2\alpha_1$, resulting in the simplified free-energy equation

$$F = \alpha_Q S^2 + \beta S^4, \qquad (6)$$

where $\alpha_Q = \alpha_0 - D^2/4\alpha_1$. Subsequent minimization of F with respect to S yields $S = \sqrt{-\alpha_Q/2\beta}$. Hence the transition temperature $T_c(H=0)$, below which helical magnetic ordering occurs, is determined by when α_Q becomes negative.

A low-temperature enhancement of the local field sensed by the muon can be achieved via an increase of S, which implies an increase in the negative value of α_Q and/or a decrease in the positive value of β. Since β originates from the spin-spin interaction, smaller β implies a stronger FM interaction between the Cr spins—although this effect would be quite small. On the other hand, a larger negative value of α_Q corresponds to a weaker DM interaction D. This will occur if there is a change in the ratio between the a (and b) and c-axis lattice constants, such that there is a rotation of the vectors $\mathbf{D}_1$, $\mathbf{D}_2$, and $\mathbf{D}_3$ towards the xy plane. Thus we propose a change in the length of one or more of the lattice constants below $T \sim 50$ K.

In conclusion, our μSR measurements reveal a possible change in the magnetic structure of $Cr_{1/3}NbS_2$ below $T \sim 50$ K, which is the same temperature region where anomalous behavior has been observed in bulk transport measurements. The low-temperature modification of the magnetic structure can be explained by a change in lattice constants, which can be confirmed by precision measurements of the crystal structure. Moreover, to confirm that the change in lattice constants is such that it causes a reduction of the DM interaction, we suggest a neutron-scattering measurement to look for a change of the ordering wave vector Q_0—since a consequence of a smaller DM interaction is a longer spin-helix period. Last, we do not find anything unusual about the magnetism near the PM transition at low field (such as phase separation) that would contribute to the anomalies observed in transport measurements near T_c.

---

[1] T. Miyadai, K. Kikuchi, H. Kondo, S. Sakka, M. Arai, and Y. Ishikawa, J. Phys. Soc. Jpn. **52**, 1394 (1983).

[2] Y. Togawa, T. Koyama, K. Takayanagi, S. Mori, Y. Kousaka, J. Akimitsu, S. Nishihara, K. Inoue, A. S. Ovchinnikov, and J. Kishine, Phys. Rev. Lett. **108**, 107202 (2012).

[3] Y. Togawa, Y. Kousaka, S. Nishihara, K. Inoue, J. Akimitsu, A. S. Ovchinnikov, and J. Kishine, Phys. Rev. Lett. **111**, 197204 (2013).

[4] N. J. Ghimire, Ph.D. thesis, University of Tennessee, 2013.

[5] A. Bornstein, Undergraduate honors thesis, University of Colorado, 2014.

[6] N. J. Ghimire, M. A. McGuire, D. S. Parker, B. Sipos, S. Tang, J.-Q. Yan, B. C. Sales, and D. Mandrus, Phys. Rev. B **87**, 104403 (2013).

[7] S. S. P. Parkin and R. H. Friend, Philos. Mag. B **41**, 95 (1980).

[8] P. Bak and M. H. Jensen, J. Phys. C **13**, L881 (1980).

[9] M. L. Plumer and M. B. Walker, J. Phys. C **14**, 4689 (1981).

[10] I. E. Dzyaloshinskii, Zh. Eksp. Teor. Fiz. **46**, 1420 (1964) [Sov. Phys. JETP **19**, 960 (1964)].